

Experimental and numerical study of the symbolic dynamics of a modulated external-cavity semiconductor laser

Andrés Aragonese,^{1,*} Taciano Sorrentino,^{1,2} Sandro Perrone,¹ Daniel J. Gauthier,³ M. C. Torrent,¹ and Cristina Masoller¹

¹Departament de Física i Enginyeria Nuclear, Universitat Politècnica de Catalunya, Colom 11, 08222 Terrassa, Barcelona, Spain

²Departamento de Ciências Exatas e Naturais, Universidade Federal Rural do Semi-Árido, 59625-900 Mossoró, Brazil

³Duke University, Physics department, Box 90305, Durham, North Carolina 27708, USA

[*andres.aragonese@upc.edu](mailto:andres.aragonese@upc.edu)

Abstract: We study the symbolic dynamics of a stochastic excitable optical system with periodic forcing. Specifically, we consider a directly modulated semiconductor laser with optical feedback in the low frequency fluctuations (LFF) regime. We use a method of symbolic time-series analysis that allows us to uncover serial correlations in the sequence of intensity dropouts. By transforming the sequence of inter-dropout intervals into a sequence of symbolic patterns and analyzing the statistics of the patterns, we unveil correlations among several consecutive dropouts and we identify clear changes in the dynamics as the modulation amplitude increases. To confirm the robustness of the observations, the experiments were performed using two lasers under different feedback conditions. Simulations of the Lang-Kobayashi (LK) model, including spontaneous emission noise, are found to be in good agreement with the observations, providing an interpretation of the correlations present in the dropout sequence as due to the interplay of the underlying attractor topology, the external forcing, and the noise that sustains the dropout events.

© 2014 Optical Society of America

OCIS codes: (140.2020)Diode lasers; (140.5960)Semiconductor lasers; (190.3100)Instabilities and chaos; (140.1540)Chaos.

References and links

1. C. Bandt and B. Pompe, "Permutation entropy: a natural complexity measure for time series," *Phys. Rev. Lett.* **88**, 174102 (2002).
2. O. A. Rosso, H. A. Larrondo, M. T. Martin, A. Plastino, and M. A. Fuentes, "Distinguishing noise from chaos," *Phys. Rev. Lett.* **99**, 154102 (2007).
3. N. Rubido, J. Tiana-Alsina, M. C. Torrent, J. Garcia-Ojalvo, and C. Masoller, "Language organization and temporal correlations in the spiking activity of an excitable laser: experiments and model comparison," *Phys. Rev. E* **84**, 026202 (2011).
4. L. Zunino, M. C. Soriano, and O. A. Rosso, "Distinguishing chaotic and stochastic dynamics from time series by using a multiscale symbolic approach," *Phys. Rev. E* **86**, 046210 (2012).
5. M. C. Soriano, L. Zunino, L. Larger, I. Fischer, and C. R. Mirasso, "Distinguishing fingerprints of hyperchaotic and stochastic dynamics in optical chaos from a delayed opto-electronic oscillator," *Opt. Lett.* **36**, 2212 (2011).
6. A. Aragonese, N. Rubido, J. Tiana-alsina, M. C. Torrent, and C. Masoller, "Distinguishing signatures of determinism and stochasticity in spiking complex systems," *Sci. Rep.* **3**, 1778 (2013).

7. D. Lenstra, B. H. Verbeek, and A. J. Den Boef, "Coherence collapse in single-mode semiconductor-lasers due to optical feedback," *IEEE J. Quantum Electron.* **21**, 6, 674–679 (1985).
8. K. Lüdge editor, *Nonlinear Laser Dynamics. From Quantum Dots to Cryptography* (Wiley-VCH, 2011).
9. D. M. Kane and K. A. Shore editors, *Unlocking Dynamical Diversity* (John Wiley & Sons, 2005).
10. S. Donati and R-H Horng, "The diagram of feedback regimes revisited," *IEEE J. Sel. Top. Quantum Electron.* **19**, 1500309 (2013).
11. M. Giudici, C. Green, G. Giacomelli, U. Nespolo, and J. R. Tredicce, "Andronov bifurcation and excitability in semiconductor lasers with optical feedback," *Phys. Rev. E* **55**, 6414 (1997).
12. A. M. Yacomotti, M. C. Eguia, J. Aliaga, O. E. Martinez, and G. B. Mindlin, "Interspike time distribution in noise driven excitable systems," *Phys. Rev. Lett.* **83**, 292 (1999).
13. T. Heil, I. Fischer, W. Elsässer, and A. Gavrielides, "Dynamics of semiconductor lasers subject to delayed optical feedback: the short cavity regime," *Phys. Rev. Lett.* **87**, 243901 (2001).
14. A. Tabaka, K. Panajotov, I. Veretennicoff, and M. Sciamanna, "Bifurcation study of regular pulse packages in laser diodes subject to optical feedback," *Phys. Rev E* **70**, 036211 (2004).
15. J. A. Reinoso, J. Zamora-Munt, and C. Masoller, "Extreme intensity pulses in a semiconductor laser with a short external cavity," *Phys. Rev. E* **87**, 062913 (2013).
16. S. D. Cohen, A. Aragoñeses, D. Rontani, M. C. Torrent, C. Masoller, and D. J. Gauthier, "Multidimensional subwavelength position sensing using a semiconductor laser with optical feedback," *Opt. Lett.* **38**, 4331 (2013).
17. L. Junges, T. Pöschel, and J. A. C. Gallas, "Characterization of the stability of semiconductor lasers with delayed feedback according to the Lang–Kobayashi model," *Eur. Phys. J. D.* **67**, 149 (2013).
18. D. W. Sukow, J. R. Gardner, and D. J. Gauthier, "Statistics of power-dropout events in semiconductor lasers with time-delayed optical feedback," *Phys. Rev. A* **56**, R3370 (1997).
19. J. Mulet and C. R. Mirasso, "Numerical statistics of power dropouts based on the Lang–Kobayashi mod," *Phys. Rev. E* **59**, 5400 (1999).
20. M. Sciamanna, C. Masoller, N. B. Abraham, F. Rogister, P. Mégret, and M. Blondel, "Different regimes of low-frequency fluctuations in vertical-cavity surface-emitting lasers," *J. Opt. Soc. Am. B* **20**, 37 (2003).
21. J. F. Martínez Avila, H. L. D. de S. Cavalcante, and J. R. Rios Leite, "Experimental deterministic coherent resonance," *Phys. Rev. Lett.* **93**, 144101 (2004).
22. Y. Hong and K. A. Shore, "Statistical measures of the power dropout ratio in semiconductor lasers subject to optical feedback," *Opt. Lett.* **30**, 3332 (2005).
23. A. Torcini, S. Barland, G. Giacomelli, and F. Marin, "Low-frequency fluctuations in vertical cavity lasers: experiments versus Lang–Kobayashi dynamics," *Phys. Rev. A* **74**, 063801 (2006).
24. J. Zamora-Munt, C. Masoller, and J. Garcia-Ojalvo, "Transient low-frequency fluctuations in semiconductor lasers with optical feedback," *Phys. Rev. A* **81**, 033820 (2010).
25. K. Hicke, X. Porte, and I. Fischer, "Characterizing the deterministic nature of individual power dropouts in semiconductor lasers subject to delayed feedback," *Phys. Rev. E* **88**, 052904 (2013).
26. D. Baums, W. Elsässer and E. O. Göbel, "Farey tree and Devil's staircase of a modulated external-cavity semiconductor laser," *Phys. Rev. Lett.* **63**, 155 (1989).
27. J. P. Toomey, D. M. Kane, M. W. Lee, and K. A. Shore, "Nonlinear dynamics of semiconductor lasers with feedback and modulation," *Opt. Express* **18**, 1695516972 (2010).
28. Y. Liu, N. Kikuchi, and J. Ohtsubo, "Controlling dynamical behavior of a semiconductor laser with external optical feedback," *Phys. Rev. E* **51**, R2697–R2700 (1995).
29. D. W. Sukow and D. J. Gauthier, "Entraining power-dropout events in an external-cavity semiconductor laser using weak modulation of the injection current," *IEEE J. Quantum Electron.* **36**, 175 (2000).
30. W-S Lam, N. Parvez, and R. Roy, "Effect of spontaneous emission noise and modulation on semiconductor lasers near threshold with optical feedback," *Int. J. of Modern Phys. B* **17**, 4123–4138 (2003).
31. J. M. Mendez, R. Laje, M. Giudici, J. Aliaga, and G. B. Mindlin, "Dynamics of periodically forced semiconductor laser with optical feedback," *Phys. Rev. E* **63**, 066218 (2001).
32. F. Marino, M. Giudici, S. Barland, and S. Balle, "Experimental evidence of stochastic resonance in an excitable optical system," *Phys. Rev. Lett.* **88**, 040601 (2002).
33. J. M. Buldú, J. Garcia-Ojalvo, C. R. Mirasso, and M. C. Torrent, "Stochastic entrainment of optical power dropouts," *Phys. Rev. E* **66**, 021106 (2002).
34. J. M. Buldú, D. R. Chialvo, C. R. Mirasso, M. C. Torrent, and J. Garcia-Ojalvo, "Ghost resonance in a semiconductor laser with optical feedback," *Europhys. Lett.* **64**, 178 (2003).
35. T. Schwalger, J. Tiana-Alsina, M. C. Torrent, J. Garcia-Ojalvo, and B. Lindner, "Interspike-interval correlations induced by two-state switching in an excitable system," *Europhys. Lett.* **99**, 10004 (2012).
36. R. Lang and K. Kobayashi, "External optical feedback effects on semiconductor injection laser properties," *IEEE J. Quantum Electron.* **16**, 347 (1980).

1. Introduction

Inferring signatures of determinism in stochastic high-dimensional complex systems is a challenging task, and much effort is focused on developing efficient and computationally fast methods of time-series analysis that are useful even in the presence of high levels of noise [1–6]. In optics, a long standing discussion about the roles of stochastic and deterministic nonlinear processes comes from the dynamics of semiconductor lasers with optical feedback. Their dynamical behavior has been studied for decades and is still the object of intense research, allowing for the observation of a great variety of phenomena [7–10], including excitability [11, 12], regular pulses [13, 14], extreme pulses and intermittency [15], quasiperiodicity [16] and chaos [17].

A particular dynamical behavior occurs for moderate feedback near the solitary laser threshold, and is referred to as low-frequency fluctuations (LFFs) [18–25]. In the LFF regime, the laser output intensity displays irregular, apparently random and sudden, dropouts. In particular, the LFF dynamics has been studied in detail when the laser current is periodically modulated [26, 27], not only because the LFFs can be controlled via current modulation [28], but also, from a complex systems perspective, because the interplay of nonlinearity, noise, periodic forcing and delayed feedback leads to entrainment and synchronization [29, 30], providing a controllable experimental setup for studying these phenomena. In addition, because the LFF dynamics is excitable, the influence of external forcing has also attracted attention from the point of view of improving our understanding of how excitable systems respond to external signals to encode information [31–35].

In this paper, we use a symbolic method of time-series analysis, referred to as ordinal analysis [1], to study the transition from the LFF dynamics of the unmodulated laser, in which the dropouts are highly stochastic and reveal only weak signatures of an underlying deterministic attractor [6], to the modulated LFF dynamics, which consists of more regular dropouts, with a periodicity that is related to external forcing period [29]. For increasing modulation amplitude there is a gradual transition from mainly stochastic to mainly deterministic behavior, and our goal is to identify in this transition characteristic features which are fingerprints of the underlying topology of the phase space of the system.

By using ordinal analysis applied to experimentally recorded sequences of inter-dropout intervals (IDIs), we identify clear changes in the symbolic dynamics as the modulation amplitude increases. Specifically, our analysis uncovers the presence of serial correlations in the sequence of dropouts, and reveals how they are modified by the amplitude of the external forcing. To demonstrate the robustness and the generality of the observations, the experiments are performed with two lasers under different feedback conditions.

We also show that simulations of the Lang-Kobayashi (LK) model [36] are in good qualitative agreement with the experimental observations. While the LK model has been shown to adequately reproduce the main statistical features of the LFF dynamics, such as the IDI distribution with and without modulation [19, 29, 30], it has also been shown that the LFFs are noise sustained in the LK model [23, 24] (*i.e.*, the LFFs are a transient dynamics that dies out when the trajectory finds a stable cavity mode, in deterministic simulations of the LK model). Therefore, it is remarkable that, in spite of the fact that the inclusion of noise is required for simulating sustained LFFs, the model adequately reproduces the symbolic dynamics, and in particular, the correlations present in the sequence of dropouts, and how they vary with the modulation amplitude.

2. Experimental setup and LFF dynamics with current modulation

The experimental setup is shown in Fig. 1: we perform the experiments with a laser emitting at 650 nm with free-space feedback provided by a mirror, and with a laser emitting at 1550 nm, with feedback provided by an optical fiber.

For the 650 nm laser, the external cavity is 70 cm (giving a feedback time delay of 4.7 ns) and the feedback threshold reduction is 8%. A 50/50 beam-splitter sends light to a photo-detector (Thorlabs DET210) connected with a 1 GHz oscilloscope (Agilent DSO 6104A). The solitary threshold is 38 mA and the current and temperature (17 C) are stabilized with an accuracy of 0.01 mA and 0.01 C, respectively, using a controller (Thorlabs ITC501). Through a bias-tee in the laser head, a sinusoidal RF component from a leveled waveform generator (HP Agilent 3325A) is combined with a constant dc current of 39 mA. The modulation frequency is $f_{mod} = 17$ MHz and the modulation amplitude varies from 0 mV to 78 mV in steps of 7.8 mV (from 0% to 4% of the dc current in steps of 0.4%). For each modulation amplitude, five measurements of 3.2 ms were recorded. The time series contains between 74,000 and 207,000 dropouts, at low and high modulation amplitude, respectively.

For the 1550 nm laser, the time delay is 25 ns and feedback threshold reduction is 10.7%. The solitary threshold is 11.20 mA, the dc value of the pump current is 12.50 mA, the modulation frequency is $f_{mod} = 2$ MHz and the modulation amplitude varies from 0 mV to 150 mV in steps of 10 mV (from 0% to 24% of the dc current in steps of 1.6%). The time series contain between 8,000 and 19,000 dropouts, at low and high modulation amplitude, respectively. While, for the 1550 nm laser, the modulation frequency is about one order of magnitude smaller than for the 650 nm laser, the relation with the characteristic time-scale of the LFF dynamics, given by the average inter-dropout interval $\langle \Delta T \rangle$ is about the same: for the 650 nm laser, $\langle \Delta T \rangle = 365$ ns and thus $\langle \Delta T \rangle \times f_{mod} = 6.2$. For the 1550 nm laser, $\langle \Delta T \rangle = 2.55 \mu s$ and $\langle \Delta T \rangle \times f_{mod} = 5.1$.

Figure 2 displays the intensity time series, the probability distribution functions (PDFs) of inter-dropout intervals, ΔT_i (IDIs), and the return maps, ΔT_i vs ΔT_{i+1} , for four modulation amplitudes for the 650 nm laser. As it has been reported in the literature the dropouts tend to occur at the same phase in the drive cycle with current modulation, and the IDIs are multiples of the modulation period [11, 29, 30]. For increasing modulation amplitude, the IDIs become progressively smaller multiples of the modulation period and, for high enough modulation amplitude, the power dropouts occur every modulation cycle [29]. Here, for the highest modulation amplitude, the PDF presents a strong peak at two times the modulation period [see Fig. 2(k)]. The return maps (third column of Fig. 2) display a clustered structure, with “islands” that correspond to the well-defined peaks observed in the PDFs, also in good agreement with previous reports [11, 29]. A similar behavior is observed with the 1550 nm laser. The plots of ΔT_{i+1} vs ΔT_i are almost symmetric, suggesting that $\Delta T_{i+1} < \Delta T_i$ and $\Delta T_{i+1} > \Delta T_i$ are equally probable; however, in Sec. 4 we will demonstrate that the modulation induces correlations in the ΔT_i sequence, induced by the modulation, which can not be inferred from these plots.

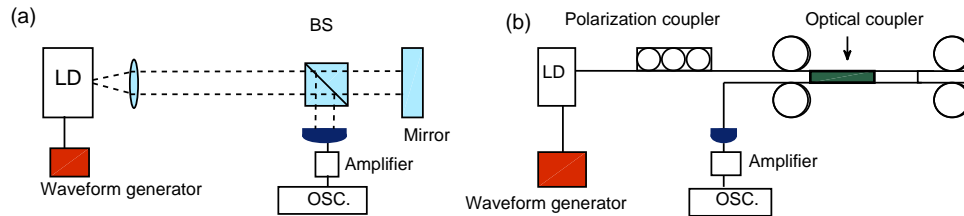


Fig. 1. Experimental setup for (a) 650 nm laser (Hitachi HL6714G) and (b) 1550 nm laser (Mitsubishi ML925B45F). LD stands for laser diode, BS for beam-splitter and OSC for oscilloscope.

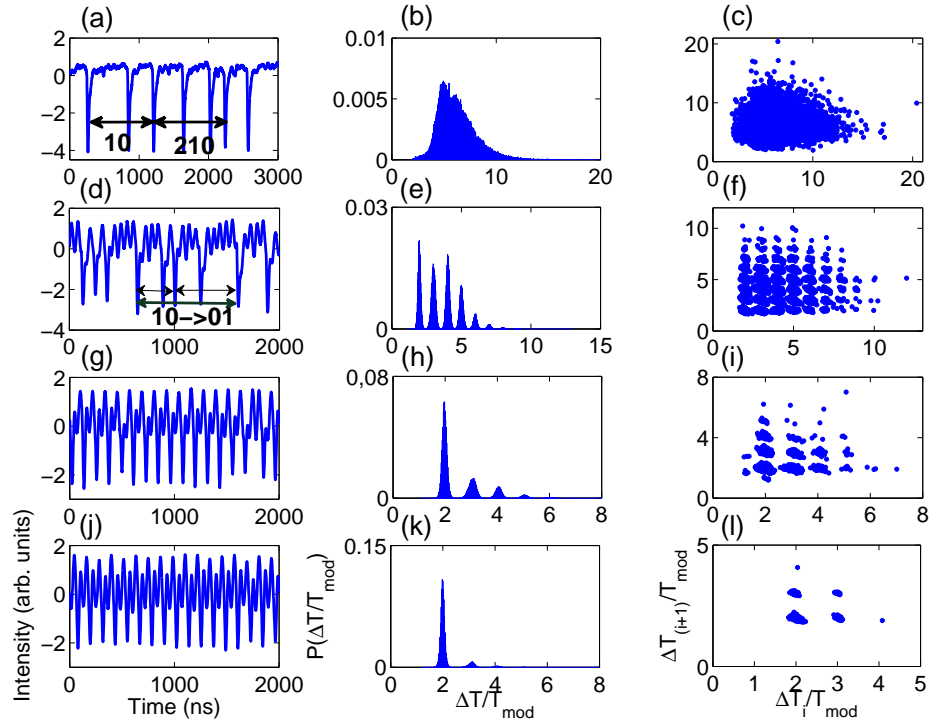


Fig. 2. Time traces of the laser intensity (650 nm laser), probability distribution functions (PDFs) of the inter-dropout intervals, ΔT_i (IDIs), and return maps (ΔT_{i+1} vs. ΔT_i) in units of the modulation period (T_{mod}) for increasing modulation amplitude: from top to bottom, No modulation, 23.4 mV (1.2%), 31.2 mV (1.6%), and 39.0 mV (2%). In panel (a) the words '10' ($D = 2$) and '210' ($D = 3$) are depicted as examples; in panel (c) the transition for '10→01' is depicted as example (see text for details).

3. Lang and Kobayashi model and method of symbolic time-series analysis

The Lang and Kobayashi (LK) rate equations for the slowly varying complex electric field amplitude E and the carrier density N are given by [36]

$$\frac{dE}{dt} = \frac{1}{2\tau_p}(1 + \alpha)(G - 1)E + \eta E(t - \tau)e^{-i\omega_0\tau} + \sqrt{2\beta_{sp}}\xi, \quad (1)$$

$$\frac{dN}{dt} = \frac{1}{\tau_N}(\mu - N - G|E|^2), \quad (2)$$

where τ_p and τ_N are the photon and carrier lifetimes respectively, α is the line-width enhancement factor, G is the optical gain, $G = N/(1 + \varepsilon|E|^2)$ (with ε being a saturation coefficient), μ is the pump current parameter, η is the feedback strength, τ is the feedback delay time, $\omega_0\tau$ is the feedback phase, and β_{sp} is the noise strength, representing spontaneous emission.

For simulating the dynamics with current modulation, the pump current parameter is $\mu = \mu_0 + a \sin(2\pi f_{mod}t)$, where a is the modulation amplitude, f_{mod} is the modulation frequency, and μ_0 is the dc current. Simulations of 2 ms were performed. The intensity time-series were averaged over a moving window of 1 ns to simulate the bandwidth of the experimental detection system. The averaged time series contained between 12,000 and 30,000 dropouts for low and

high modulation amplitude, respectively. The best agreement with the dynamics found in the experimental data was for $\mu_0 = 1.01$, $f_{mod} = 21$ MHz, $\varepsilon = 0.01$, $k = 300$ ns⁻¹, $\tau = 5$ ns, $\gamma = 1$ ns⁻¹, $\beta_{sp} = 10^{-4}$ ns⁻¹, $\eta = 10$ ns⁻¹, and $\alpha = 4$. For these parameters $\langle \Delta T \rangle = 127$ ns and $\langle \Delta T \rangle \times f_{mod} = 2.7$.

The experimental and numerical sequences of IDIs are analyzed by means of ordinal analysis [1], in which the IDI sequence is transformed into a sequence of ordinal patterns (OPs), also referred to as words. Words of length D are defined by considering the relative length of D consecutive IDIs [see Fig. 2(a)]. For $D = 2$ there are two OPs: $\Delta T_i < \Delta T_{i+1}$ gives word ‘01’ and $\Delta T_i > \Delta T_{i+1}$ gives word ‘10’; for $D = 3$ there are six OPs: $\Delta T_i < \Delta T_{i+1} < \Delta T_{i+2}$ gives ‘012’, $\Delta T_{i+2} < \Delta T_{i+1} < \Delta T_i$ gives ‘210’, etc. This symbolic transformation keeps the information about correlations present in the dropout sequence, but neglects the information contained in the duration of the IDIs. The words are formed by consecutive non-superposing IDIs (*i.e.*, for $D = 2$, $\Delta T_i, \Delta T_{i+1}$ define one word and $\Delta T_{i+2}, \Delta T_{i+3}$ define the next one). Then, the probabilities of the different words are computed in each time series.

In order to select the optimal length of the words for the analysis, we need to consider the length of the correlations present in the time-series: if D is much longer than the correlation length, most words will appear in the sequence with similar probabilities. In addition, we need to consider the length of the time-series, because the number of possible words increases with D as $D!$, and for large D values, long time series will be needed for computing the word probabilities with robust statistics. Here, we recorded long time series of dropouts and the main limitation for the value of D comes from the large level of stochasticity of the LFF dynamics, which results in correlations among only few consecutive dropouts. Thus, we limit the ordinal analysis to $D = 2$ and $D = 3$ words. We will show that the LFF symbolic dynamics is such that the analysis with words of $D = 3$ allows us to uncover correlations which are not seen with $D = 2$ words.

From the sequence of words, additional information can be extracted by computing the transition probabilities (TPs) [3] from one word to the next. In Fig. 2(d), the transition $10 \rightarrow 01$ is depicted as example. With $D = 2$ words, the TP analysis can uncover correlations among five consecutive dropouts, and thus allows us to extract information about the memory of the system in a longer time scale. The TPs can be normalized in two different ways: normalized for all transitions, such that the sum of all possible TPs is one, $\sum_{i,j} TP_{i \rightarrow j} = 1$, or normalized for each word i , such that $\sum_j TP_{i \rightarrow j} = 1 \forall i$. We compute these two sets of TPs corresponding to $D = 2$ words. For the first set, the TPs are normalized such that $TP_{(01 \rightarrow 01)} + TP_{(01 \rightarrow 10)} = 1$ and $TP_{(10 \rightarrow 01)} + TP_{(10 \rightarrow 10)} = 1$. For the second set: $TP_{(01 \rightarrow 01)}^* + TP_{(01 \rightarrow 10)}^* + TP_{(10 \rightarrow 01)}^* + TP_{(10 \rightarrow 10)}^* = 1$, and $TP_{(01 \rightarrow 10)}^* = TP_{(10 \rightarrow 01)}^*$.

4. Results

Figure 3 shows the probabilities of words of $D = 2$ (a, b, c) and $D = 3$ (d, e, f), vs. the modulation amplitude, for the 650 nm laser (a, d), for the 1550 nm laser (b, e), and for the simulated time series (c, f). The gray region indicates probability values consistent with the null hypothesis (NH) that the words are equally probable, and thus, that there are no correlations among the dropouts. In other words, probability values outside the gray regions are not consistent with a uniform distribution of word probabilities and reveal serial correlations in the IDI sequence. It can be noticed that the gray region is narrower in (a, d) than in (b, e) and (c, f). This is due to the fact that the number of dropouts recorded for the 650 nm laser is much larger than for the 1550 nm laser (the corresponding delay times being 4.7 ns and 25 ns respectively), and is also larger than the number of dropouts in the simulated data.

It is observed that the dynamics is consistent with the NH, in the case of $D = 2$, for small and for high modulation amplitude. However, the analysis with $D = 3$, reveals that, for high

modulation, the probabilities are outside the gray region, revealing correlations among four consecutive IDIs. We note that there are two groups of words, one less probable ('012', '210') and one more probable ('021', '102', '120', '201'), resulting, for $D = 2$, in the same probabilities for '01' as for '10'. With $D = 3$, the less probable words are those which imply three consecutively increasing or decreasing IDIs and this can be understood in the following terms: strong enough modulation forces a rhythm in the LFF dynamics, and three consecutively increasing or decreasing intervals imply a loss of synchrony with the external rhythm, and thus, are less likely to occur.

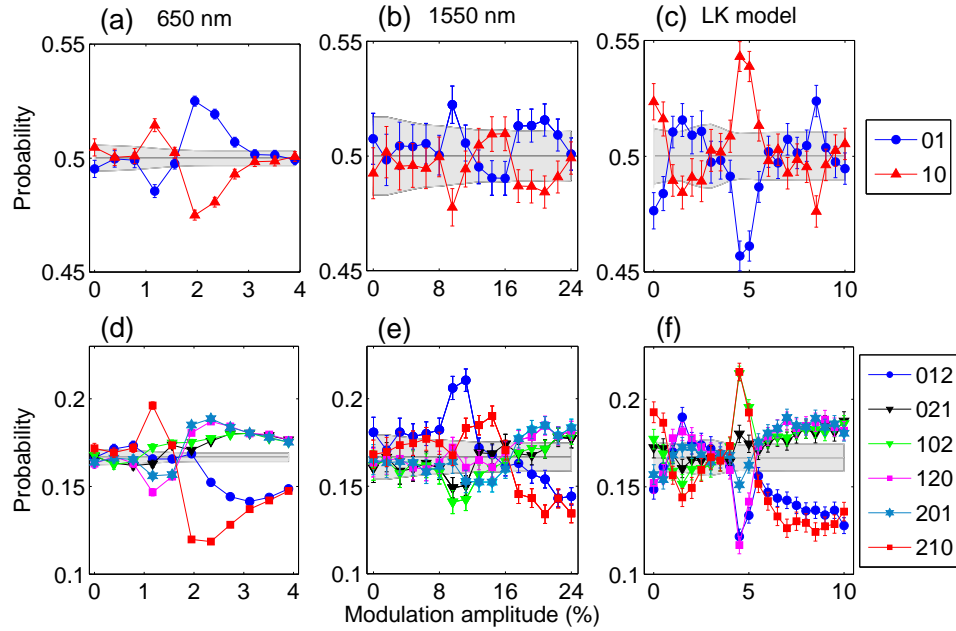


Fig. 3. Probabilities of the words of $D = 2$ (a, b, c) and $D = 3$ (d, e, f) versus the modulation amplitude for the experiment with the 650 nm laser (a, d), the experiment with the 1550 nm laser (b, e), and the numerical simulations of the LK model (c, f). The gray region ($p \pm 3\sigma$, where $p = 1/D!$, $\sigma = \sqrt{p(1-p)/N}$, and N is the number of words in the symbolic sequence) indicates probability values consistent with 95% confidence level with the null hypothesis that all the words are equally probable (*i.e.*, that there are no correlations present in the sequence of dropouts).

By computing the four transition probabilities of $D = 2$ words, depicted in Fig. 4, we obtain information about correlations among five consecutive dropouts. This analysis is statistically more robust than computing the probabilities of the 24 words of length $D = 4$.

The results in Fig. 4 confirm that, at this time scale, the dynamics is still consistent with the NH for low modulation amplitudes but, as the modulation increases, a transition takes place and the TPs display a deterministic-like behavior. This transitions occur at the same values as in Fig. 3 (at about 1.8% modulation amplitude for the 650 nm case, 16% for the 1550nm case, and 6% for the simulated data). Figure 4 shows that, for high modulation amplitude, the most probable transitions are those which go from one word to the same word ('01 \rightarrow 01' and '10 \rightarrow 10'), because the external forcing imposes a periodicity in the LFF dynamics. The transition in the dynamics, and the qualitative agreement between experiments and simulations, are independent of the type of normalization used to compute the TPs.

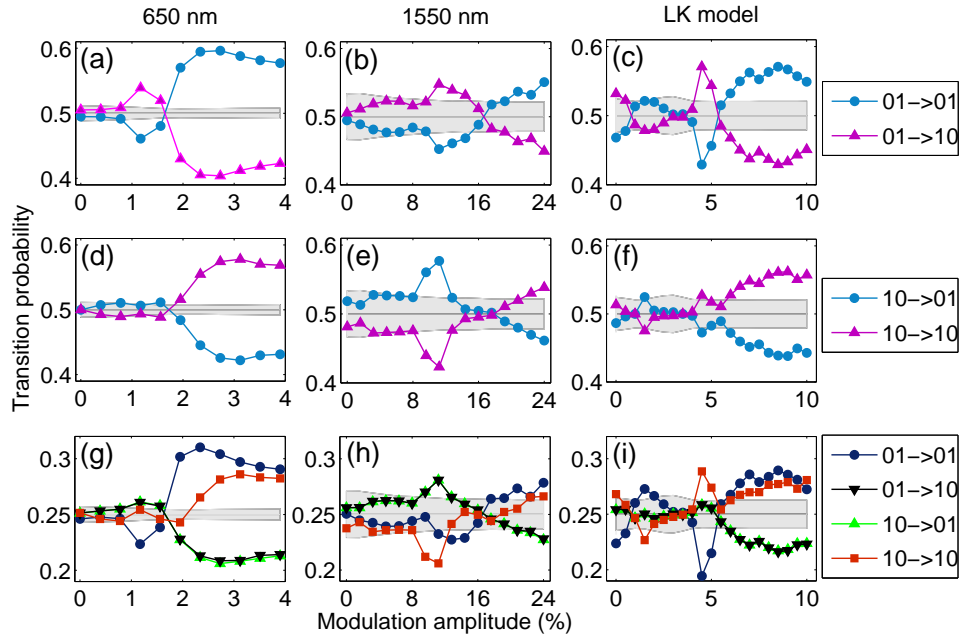


Fig. 4. Transition probabilities for the 650 nm laser (a, d, g), the 1550 nm laser (b, e, h), and the simulated data (c, f, i). The first row indicates the transition probabilities from word '01' to '01' and '10', such that $TP_{(01 \rightarrow 01)} + TP_{(01 \rightarrow 10)} = 1$. The second row indicates the transition probabilities from word '10' to '01' and '10', such that $TP_{(10 \rightarrow 01)} + TP_{(10 \rightarrow 10)} = 1$, while the third row considers all four transitions, such that $TP_{(01 \rightarrow 01)}^* + TP_{(01 \rightarrow 10)}^* + TP_{(10 \rightarrow 01)}^* + TP_{(10 \rightarrow 10)}^* = 1$.

In Figs. 3 and 4, there is a good qualitative agreement between experiments and simulations. As discussed in the introduction, within the framework of the LK model, the LFF dynamics is sustained by spontaneous emission noise, and thus, one could expect weak correlations in the sequence of dropouts. While this is indeed the case for no modulation or very weak modulation amplitude, larger modulation induces precise correlations, which are adequately reproduced by the LK model. For strong modulation the reason why some words and transitions are more probable than the others is well understood (as due to the external rhythm imposed by the modulation), but for no modulation and also for moderate modulation amplitude, further investigations are needed in order to understand the symbolic behavior. We note that, without modulation, while in the experimental data the word probabilities are within the NH gray region, in the simulated data they are not. This can be due to a number of model parameters that can be tuned in order to obtain a better fit of the symbolic dynamics without modulation (e.g., the feedback strength, the linewidth enhancement factor, the dc value of the pump current, etc.). However, our goal here is to analyze the influence of the modulation on the LFF symbolic dynamics, and a detailed comparison experiments-simulations in the absence of modulation will be reported elsewhere.

5. Conclusions

We have studied experimentally and numerically the symbolic dynamics of a semiconductor laser with optical feedback and current modulation in the LFF regime. We have analyzed time

series of inter-dropout intervals employing a symbolic transformation that allows us to identify clear changes in the dynamics induced by the modulation. For weak modulation the sequence of dropouts is found to be mainly stochastic, while for increasing modulation it becomes more deterministic, with correlations among several consecutive dropouts. We have identified clear changes in the probabilities of the symbolic words and transitions with increasing modulation amplitude. The LK model has also been tested and we have found a good qualitative agreement with the experimental observations. We speculate that the symbolic behavior uncovered here is a fingerprint of the underlying topology of the phase space, and is due to the interplay of noise-induced escapes from a stable external cavity mode, and the dynamics in the coexisting attractor. It would be interesting for a future study to analyze the influence of varying the modulation frequency and the noise strength. It would also be interesting to use an analytic effective potential [18], to further understand the mechanisms underlying the symbolic dynamics of the modulated LFFs.

The methodology proposed here can be a useful tool for identifying signatures of determinism in high-dimensional and stochastic complex systems. It provides a computationally efficient way to unveiling structures and transitions hidden in the time series. As the laser in the LFF regime is an excitable system, our results could be relevant for understanding serial correlations in the spike sequences of other forced excitable systems. Also as a future study, an analysis of simpler models of excitable systems (such as the FitzHugh-Nagumo model or the phenomenological LFF model proposed by Yacomotti et al. [12]), can contribute to improve our understanding of the symbolic behavior induced by periodic modulation.

Acknowledgments

This work was supported in part by grant FA8655-12-1-2140 from EOARD US, grant FIS2012-37655-C02-01 from the Spanish MCI, and grant 2009 SGR 1168 from the Generalitat de Catalunya. C. M. gratefully acknowledges partial support from the ICREA Academia programme. D. J. G. gratefully acknowledges the financial support of the U.S. Army Research Office through Grant W911NF-12-1-0099.